International Journal of Bifurcation and Chaos, Vol. 13, No. 4 (2003) 1–16

SYNCHRONIZATION OF COUPLED EXTENDED DYNAMICAL SYSTEMS: A SHORT REVIEW

DAMIÁN H. ZANETTE and LUIS G. MORELLI
Consejo Nacional de Investigaciones Científicas y Técnicas
Centro Atómico Bariloche and Instituto Balseiro
8400 Bariloche, Río Negro, Argentina

Received October 18, 2001

We briefly review the synchronization properties of cross-coupled spatially extended dynamical systems, with particular emphasis on elementary cellular automata and Kauffman networks subject to stochastic coupling. We also discuss the main results for the joint evolution of deterministically cross-coupled Ginzburg–Landau equations and neural networks. Both numerical and analytical approaches are addressed, and the main differences with the synchronization of zero-dimensional systems are highlighted. New results are presented characterizing the critical behavior at the synchronization transition of coupled Kauffman networks.

Keywords: Author to supply.

1. Introduction: Synchronization of Dynamical Systems

Spontaneous synchronization — namely, the temporal self-organization of the activity of interacting dynamical elements — is observed in a wide class of natural systems. Probably the first reported observation of a synchronization phenomenon is due to Christiaan Huygens who, in 1665, noticed that the pendulums of two clocks hanging close to each other from the same wall synchronize their oscillations [Strogatz & Stewart, 1993]. Though this first observation of synchronization concerns a mechanical system, the most remarkable instances of synchronous behavior in Nature are found in the living world. The synchrony of heart cells, for example, is a vital mechanism in the function of animal organisms. Neural activity in the brain is also well known to display different regimes of synchrony. They can be associated with pathological states — such as in epileptic seizures, where the activity of vast zones of the brain becomes synchronous — or with normal functions, related to the codification of information and memory [Abarbanel *et al.*, 1996]. At the level of biological populations, insect swarms exhibit some noticeable forms of synchronized collective behavior, the best known examples being the synchronous flashing fireflies [Buck & Buck, 1976] and chirping crickets [Walker, 1969]. Weaker manifestations of synchronization have also been detected in more evolved social species, including *Homo sapiens* [Winfree, 1980; Néda *et al.*, 2000].

From a more abstract viewpoint, synchronization has been identified as a generic form of collective behavior in ensembles of dynamical systems with long range coupling. Several models that capture the essence of synchronization phenomena have been thoroughly studied during the last few decades. Kuramoto [1984], for instance, has analyzed an ensemble of N coupled phase oscillators, governed by the equations

$$\dot{\phi}_i(t) = \Omega_i + \frac{\varepsilon}{N} \sum_{j=1}^{N} \sin(\phi_j - \phi_i)\,, \qquad (1)$$

$i = 1, \ldots, N$, where $\varepsilon > 0$ is the strength of coupling. In the absence of coupling, $\varepsilon = 0$, each

oscillator i performs uniform angular motion with its natural frequency Ω_i. For $\varepsilon \neq 0$ the oscillators are globally coupled, in the sense that the strength of the pair interaction does not depend on their relative position, but only on their relative state. Note, in fact, that Eq. (1) can be rewritten as

$$\dot{\phi}_i(t) = \Omega_i + \varepsilon(\cos\,\phi_i\,\overline{\sin\,\phi} - \sin\,\phi_i\,\overline{\cos\,\phi})\,, \qquad (2)$$

where overlined quantities stand for instantaneous averages over the whole system. In other words, each oscillator interacts with the rest of the system through global averages only.

Kuramoto has shown that, in the limit $N \to \infty$, there exists a critical value ε_c of the coupling intensity such that, for $\varepsilon > \varepsilon_c$, a subensemble of oscillators becomes entrained in periodic orbits with the same frequency Ω, whereas the other oscillators remain unsynchronized. If the distribution of natural frequencies $g(\Omega_i)$ is symmetric around a certain value Ω_0, the entraining frequency is precisely $\Omega = \Omega_0$, and the entrained oscillators are those whose natural frequencies are sufficiently close to Ω_0,

$$|\Omega_i - \Omega_0| \leq \varepsilon\sqrt{\frac{8g(\Omega_0)(\varepsilon - \varepsilon_c)}{\varepsilon_c^3 g''(\Omega_0)}}\,, \qquad (3)$$

where g'' stands for the second derivative of g. The critical coupling at which synchronization sets on is $\varepsilon_c = 2/\pi g(\Omega_0)$. The nature of the bifurcation at that point depends on the sign of $g''(\Omega_0)$. It is supercritical if the second derivative is negative, and subcritical if the second derivative is positive [Kuramoto, 1984].

A great deal of attention has been paid to the synchronization of ensembles formed by identical elements, especially, in the case where the individual dynamics is chaotic. Both continuous and discrete-time dynamics have been considered. Kaneko [1989; see also Kaneko, 1994 and references therein] has introduced globally coupled chaotic maps as a mean-field model of lattice maps, which are extensively used to model complex extended systems [Kaneko, 1993]. For an ensemble of N maps whose individual dynamics is governed by the equation $\mathbf{w}(t+1) = \mathbf{f}[\mathbf{w}(t)]$, global coupling is introduced as

$$\begin{aligned}\mathbf{w}_i(t+1) &= (1-\varepsilon)\mathbf{f}[\mathbf{w}_i(t)] + \frac{\varepsilon}{N}\sum_{j=1}^{N}\mathbf{f}[\mathbf{w}_j(t)] \\ &= (1-\varepsilon)\mathbf{f}[\mathbf{w}_i(t)] + \varepsilon\overline{\mathbf{f}(\mathbf{w})}\,, \qquad (4)\end{aligned}$$

$i = 1, \ldots, N$, with $\varepsilon \in [0, 1]$. While for $\varepsilon = 0$ the elements evolve independently, for $\varepsilon = 1$ they become fully synchronized after the first time step. *Full synchronization* is here understood as a situation where the individual states of all the elements in the ensemble coincide, i.e. where the trajectory of the system in phase space is restricted to the subspace $\mathbf{w}_1 = \mathbf{w}_2 = \cdots = \mathbf{w}_N$. In this situation, the evolution of all the elements coincides with that of an independent element. The state of full synchronization can be asymptotically approached as the system evolves even for $\varepsilon < 1$. It has been shown that, if the individual dynamics is chaotic, full synchronization is linearly stable for $\varepsilon > \varepsilon_c$, where the critical value ε_c is related to the maximal Lyapunov exponent λ_M of the individual dynamics, as $\varepsilon_c = 1 - \exp(-\lambda_M)$. For nonchaotic individual dynamics, where $\lambda_M < 0$, full synchronization is a stable state for any $\varepsilon > 0$. The connection between ε_c and λ_M makes it clear that the transition to full synchronization in chaotic systems, which has the character of a critical phenomenon, results from the competition between the stabilizing effect of global coupling and the inherent instability of chaotic orbits. Note carefully that the critical value ε_c does not depend on N, so that the synchronization threshold is the same for any size of the coupled ensemble.

For coupling strengths just below ε_c the system evolves asymptotically to a state of partial synchronization in the form of *clustering*, where the elements become divided into groups [Kaneko, 1989]. Within each cluster the elements are fully synchronized but different clusters have different trajectories. For large systems, the dynamics in the clustering regime is highly multistable and exhibits glassy-like features [Crisanti *et al.*, 1996; Manrubia & Mikhailov, 2001]. In contrast with the critical value ε_c, the stability properties of the clustering regime are strongly dependent on the system size [Abramson, 2000]. At even lower coupling strengths the elements do not form clusters, but their interaction gives rise to unusual statistical properties in the average of dynamical quantities, specifically, in the dependence of the global average $\overline{\mathbf{f}(\mathbf{w})}$ on the system size N [Kaneko, 1990; Perez *et al.*, 1992, 1993]. It has been shown that the mean square dispersion over time, $\sigma = \langle(\overline{\mathbf{f}(\mathbf{w})} - \langle\overline{\mathbf{f}(\mathbf{w})}\rangle)^2\rangle^{1/2}$, does not satisfy the law of large numbers, i.e. $\sigma \not\sim N^{1/2}$, but grows much slowly with N.

Similar features have been analyzed in ensembles of continuous-time dynamical elements. If the

individual dynamics is given by $\dot{\mathbf{w}} = \mathbf{F}(\mathbf{w})$, global coupling can be introduced as [Fujisaka & Yamada, 1983]

$$\begin{aligned}\dot{\mathbf{w}}_i &= \mathbf{F}(\mathbf{w}_i) + \frac{\varepsilon}{N}\sum_{j=1}^{N}(\mathbf{w}_j - \mathbf{w}_i) \\ &= \mathbf{F}(\mathbf{w}_i) + \varepsilon(\overline{\mathbf{w}} - \mathbf{w}_i)\,, \end{aligned} \tag{5}$$

$i = 1, \ldots, N$, with $\varepsilon > 0$. Coupling acts as a relaxation mechanism of the individual dynamics towards the average state $\overline{\mathbf{w}}$. With this interaction, usually referred to as "vector" coupling [Heagy *et al.*, 1994], full synchronization becomes linearly stable at a critical coupling strength $\varepsilon_c = \lambda_M$ where, as before, λ_M is the maximal Lyapunov exponent of the individual dynamics [Fujisaka & Yamada, 1983; Heagy *et al.*, 1994]. For nonchaotic dynamics full synchronization is linearly stable for any $\varepsilon > 0$. Other forms of global coupling for continuous-time dynamical systems have been proposed, for which global stability of full synchronization above a certain threshold can be proven [Zanette & Mikhailov, 1998a]. Such as for globally coupled maps, full synchronization in continuous-time systems is preceded by a regime of clustering, which has been statistically characterized for ensembles of chaotic Rössler oscillators [Zanette & Mikhailov, 1998a; 2000]. The effect of noise in this kind of dynamical systems has also attracted attention [Zanette & Mikhailov, 2000], in view of its relevance in experimental realizations of coupled chaotic oscillators [Wang *et al.*, 2000].

In this paper, we review the synchronization properties of a special kind of dynamical systems, namely, extended systems. As explained in the next section, extended systems are spatially distributed ensembles of interacting dynamical elements. We shall however be not interested in the synchronized behavior of the elements inside a *single* extended system, but in the mutual synchronization of *two* interacting (cross-coupled) extended systems. Particular attention will be paid to a special class of discrete extended systems, namely, cellular automata and, in particular, to Kauffman networks (Sec. 3), for which the synchronization transition can be studied analytically. Other kinds of extended systems are considered in Sec. 4.

2. Cross-Coupled Extended Systems

Extended systems are dynamical systems where the state variable $\mathbf{w}$ depends not only on time, but on a set of additional independent variables $\mathbf{x}$, $\mathbf{w} \equiv \mathbf{w}(\mathbf{x}, t)$. These new variables are typically interpreted as spatial coordinates, in particular, when there is a metric structure associated with them. An extended system can generally be thought of as a set of zero-dimensional dynamical elements distributed over space, whose individual dynamics influence each other through an interaction which usually depends on the distance between elements. The generic evolution equation for an extended system can be written as

$$\partial_t \mathbf{w} = \mathcal{F}[\mathbf{w}(\mathbf{x}, t)]\,, \tag{6}$$

where, in general, the operator $\mathcal{F}$ acts on the spatial variable $\mathbf{x}$, for example, through gradients or integrals. Probably the simplest instance of an extended system of this class is given by the wave equation

$$\partial_t \mathbf{w} + (\mathbf{v}\cdot\nabla)\mathbf{w} = 0\,, \tag{7}$$

whose general solution — in the absence of boundary constraints — is $\mathbf{w}(\mathbf{x}, t) = \mathbf{w}(\mathbf{x} - \mathbf{v}t)$. This solution represents the shape-preserving propagation of a perturbation $\mathbf{w}(\mathbf{x}, 0)$ at velocity $\mathbf{v}$. Another well-known instance is that of reaction–diffusion systems,

$$\partial_t \mathbf{w} = D\nabla^2\mathbf{w} + \mathbf{F}(\mathbf{w})\,. \tag{8}$$

This equation describes a distributed continuous set of active elements whose individual dynamics is given by $\dot{\mathbf{w}} = \mathbf{F}(\mathbf{w})$, interacting through diffusive coupling between (infinitely) near neighbors. Reaction–diffusion models have been extensively used to describe pattern formation in physicochemical systems [Mikhailov, 1994], but also play a key role in the understanding of morphogenesis in living organisms and of the dynamics of interacting biological species [Murray, 1993].

In connection with different applications, extended systems where the variable $\mathbf{x}$ varies over a discrete set constitute another important class. The paradigm of this class is given by neural networks [Mikhailov, 1994], which are discrete, but typically large, ensembles of dynamical elements — the neurons — with specific kinds of interactions. Discretization of variables is a convenient way to simplify the study of complex systems, especially, from the viewpoint of numerical analysis. As a matter of fact, fully discretized extended systems — namely, cellular automata, where time, space,

and the internal state vary over discrete sets — were already well known two decades ago [Wolfram, 1983]. Cellular automata were initially introduced to mimic self-reproducing machines and as universal computers. After the work by Wolfram [1986], who conjectured that the laws of nature could be given in terms of such fully discretized entities, they have been extensively applied to model physical, biological and artificial systems.

A cellular automaton consists of a spatial array of discrete elements — the cells. The state $\sigma_i(t)$ of each element adopts, at each time step t, a value taken from a fixed discrete set. The state of the whole automaton at a given time is specified by the vector $\boldsymbol{\sigma} = (\sigma_1, \sigma_2, \ldots, \sigma_N)$, where N is the system size. The evolution of each cell i is determined by the state of the cells in its neighborhood $\mathcal{N}_i$. Namely, $\sigma_i(t+1)$ is a function of $\sigma_j(t)$ with $j \in \mathcal{N}_i$. As an explicit example, we consider the so-called elementary cellular automata. These are one-dimensional arrays of cells with binary states, $\sigma_i \in \{0, 1\}$, where the neighborhood of each cell is formed by itself and its two nearest neighbors. Periodic boundary conditions, $i + N \equiv i$, are usually assumed. The evolution rule is homogeneous along the array, and thus can be written as

$$\sigma_i(t+1) = f[\sigma_{i-1}(t), \sigma_i(t), \sigma_{i+1}(t)]\,, \qquad (9)$$

where f is a Boolean function. The state of all sites is updated simultaneously. Note that, since the state of each cell has two possible values and each neighborhood contains three cells, the total number of possible evolution rules for elementary cellular automata is $2^{(2^3)} = 256$. Systematic study of cellular automata has shown that they are able to exhibit very complex forms of evolution [Herrmann, 1989], whose characterization, in fact, has still to be completely achieved. Even for elementary cellular automata a wide variety of behaviors has been observed [Wolfram, 1983; Herrmann, 1989], depending on the form of the evolution rule f. Some of them can exhibit nonperiodic evolution in the limit $N \to \infty$, displaying spatiotemporal structures that mimic those observed in chaotic extended systems.

Kauffman networks, also known as random Boolean networks, are closely related to cellular automata. They were introduced as a model for the problem of cell differentiation [Kauffman, 1969, 1984, 1993]. Since then, they have been the object of many studies concerning their properties [Derrida & Pomeau, 1986; Derrida & Weisbuch, 1986; Flyvbjerg, 1988; Kauffman, 1993; Bastolla & Parisi, 1996, 1998a, 1998b] and have been extensively applied as models of biological evolution. A Kauffman network is an N-site network where each site is connected to K randomly chosen sites, which constitute its neighborhood. As in elementary cellular automata, the state of each site is given by a Boolean variable $\sigma_i \in \{0, 1\}$, and evolves according to the inputs coming from its neighborhood. The evolution rule is chosen independently and randomly for each site. To each of the 2^K possible configurations of the neighborhood of each site an output is assigned, namely, 1 with probability p, or 0 with probability $1 - p$. The probability p is referred to as the *bias* of the network. The state of all sites is updated simultaneously according to the corresponding functions. The K connections and the evolution rule of each site are chosen at the beginning and kept fixed during the evolution. Thus, the disorder is quenched and, as in cellular automata, the dynamics is deterministic. In the (K, p) parameter space, Kauffman networks present phases of frozen and active evolution. Whereas for small K all sites converge to static states or to cycles of short period, for large K very long cycles are typically observed. As $N \to \infty$, the period of these cycles may diverge and the evolution becomes chaotic. The transition between the two phases, which occurs at $K = [2p(1-p)]^{-1}$, has been extensively studied [Derrida & Pomeau, 1986; Derrida & Weisbuch, 1986; Flyvbjerg, 1988].

In summary, extended dynamical systems provide a versatile collection of models for a wide class of complex natural phenomena, ranging from pattern formation in physicochemical reactions, to biological morphogenesis, to evolutionary processes. It is therefore interesting to consider how these systems behave under the effect of mutual interactions and, in particular, study the synchronization properties of their coevolution when they are mutually coupled by algorithms similar to those discussed in the Introduction for zero-dimensional systems.

The scheme of coupling introduced in Eq. (5) can be straightforwardly extended to the case of an ensemble of identical extended systems of type (6), as

$$\partial_t \mathbf{w} = \mathcal{F}[\mathbf{w}] + \varepsilon(\overline{\mathbf{w}} - \mathbf{w}_i)\,, \qquad (10)$$

where $\overline{\mathbf{w}} = N^{-1} \sum_j \mathbf{w}_j$. This scheme is formally equivalent to the vector coupling of Eq. (5). We point out, however, that in (10) mutual interaction of the extended systems couples the variables $\mathbf{w}_i$

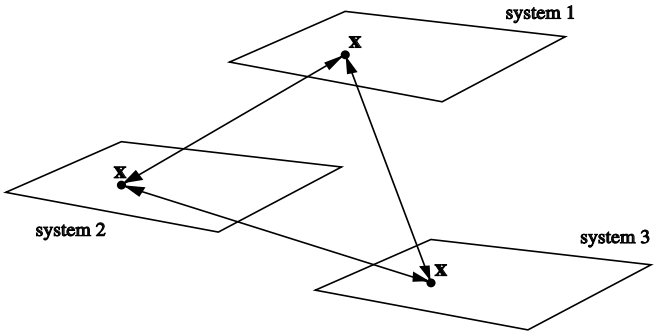

Fig. 1. Global cross-coupling of three identical extended systems.

at the same values of $\mathbf{x}$ only. In other words, only *homologous* elements of the extended systems interact with each other, as schematically shown in Fig. 1. This interaction is referred to as global *cross-coupling*.

Let us illustrate the effect of this interaction by considering two cross-coupled one-dimensional wave equations,

$$\begin{aligned} \partial_t w_1 + v\partial_x w_1 &= \varepsilon(w_2 - w_1)/2\,, \\ \partial_t w_2 + v\partial_x w_2 &= \varepsilon(w_1 - w_2)/2. \end{aligned} \tag{11}$$

The quantities $w_1(x,t)$ and $w_2(x,t)$ can be interpreted as the densities of two chemicals A_1 and A_2 being advected at velocity v, and undergoing the reversible isomeric reaction $A_1 \leftrightarrow A_2$ at rate $\varepsilon/2$. The density difference $u = w_2 - w_1$ satisfies the equation

$$\partial_t u + v\partial_x u = -\varepsilon u\,, \tag{12}$$

whose solution for the initial condition $u(x,0)$ is

$$u(x,t) = u(x - vt, 0)\, \exp(-\varepsilon t)\,. \tag{13}$$

This represents a propagating field affected by exponential damping at rate ε. At asymptotically long times, $u(x,t) \to 0$ for all x. This implies that the evolution of the two fields w_1 and w_2 becomes synchronized, in the sense that $w_1(x,t) = w_2(x,t)$ for $t \to \infty$. Figure 2 shows four stages in the evolution towards synchronization of two propagating pulses coupled as in (11). We see that, in agreement with the behavior of coupled nonchaotic zero-dimensional dynamical elements, these two extended systems synchronize for any positive value of the coupling intensity ε. In order to study the case of chaotic extended systems, it is convenient to analyze coupled cellular automata and Kauffman networks, which are particularly suitable for

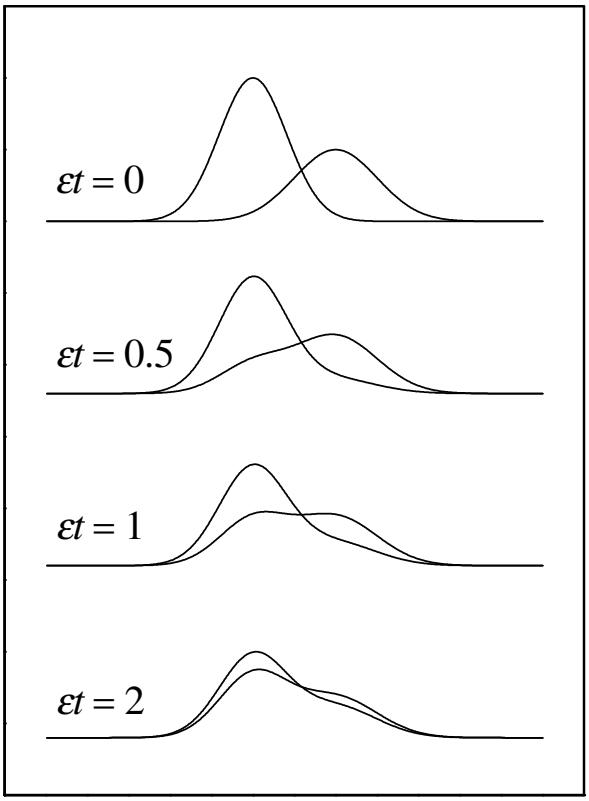

Fig. 2. Four snapshots of the evolution of two propagating pulses coupled as in Eq. (11).

numerical treatment. Due to the fully discretized dynamics of this systems, however, it is necessary to modify the coupling algorithm. In the next section, a form of stochastic coupling for cellular automata and Kauffman networks is described, and their synchronization properties — resulting from numerical and analytical study — are discussed.

3. Synchronization of Cellular Automata and Kauffman Networks

Cellular automata and Kauffman networks constitute a useful tool to explore, both numerically and analytically, the properties of coupled extended dynamical systems. We recall that they consist of ensembles of cells whose individual states vary by discrete steps on a discrete set, and are determined by prescribed Boolean functions of the state of the neighboring cells. As advanced above, due to the discrete nature of cellular automata and Kauffman networks — which, from now on, we generically refer to as automata — it is not possible to introduce a form of deterministic coupling able to be controlled with a continuous parameter such as the

coupling intensity ε of Eq. (10). One can use instead a form of stochastic coupling, characterized by a probability q ($0 \leq q \leq 1$), as follows [Morelli & Zanette, 1998; Bagnoli & Rechtman, 1999; Grassberger, 1999]. At each time step, the dynamics of the two coupled automata, whose individual states are respectively denoted $\boldsymbol{\sigma}^1$ and $\boldsymbol{\sigma}^2$, is given by the successive action of the individual evolution $\mathbf{f}(\boldsymbol{\sigma})$ [cf. Eq. (9)], and a stochastic coupling operator $\mathcal{S}$, whose definition is introduced below:

$$\boldsymbol{\sigma}^{1,2}(t+1) = \mathcal{S} \circ \mathbf{f}[\boldsymbol{\sigma}^{1,2}(t)] \,. \tag{14}$$

The operator $\mathcal{S}$ compares the states σ_i^1 and σ_i^2 of the homologous cells in each automaton for all i. If $\sigma_i^1 = \sigma_i^2$, both states are kept invariant. Otherwise, with probability $1-q$ they are also left unchanged, but with the complementary probability q, the states are made equal either to σ_i^1 or to σ_i^2. This latter choice is made with probability 1/2. Therefore:

$$\mathcal{S}_i(\boldsymbol{\sigma}^{1,2}) = \begin{cases} \sigma_i^{1,2} & \text{if } \sigma_i^1 = \sigma_i^2 \,, \\ \sigma_i^{1,2} & \text{with probability } 1-q, \text{ if } \sigma_i^1 \neq \sigma_i^2 \,, \\ \sigma_i^1 & \text{with probability } q/2, \text{ if } \sigma_i^1 \neq \sigma_i^2 \,, \\ \sigma_i^2 & \text{with probability } q/2, \text{ if } \sigma_i^1 \neq \sigma_i^2 \,. \end{cases} \tag{15}$$

This form of coupling, in which the states of homologous cells are occasionally made equal, adapts to the discrete evolution of these systems the process of mutual relaxation implied by the coupling terms of Eqs. (5) and (10).

When the coupling probability q vanishes, the two automata evolve independently of each other. From different random initial conditions — and except for a few trivial evolution rules — their states will always differ to some extent. On the other hand, for $q = 1$, the two automata are fully synchronized after the first evolution step. From then on, they will reproduce the evolution of an uncoupled automaton but their states will be mutually identical. From comparison with the behavior of deterministically coupled dynamical systems, described in the previous sections, this circumstance suggests that a synchronization transition occurs in the interval $0 < q < 1$. We however point out that, due to the different nature of deterministic and stochastic coupling, the implication is not straightforward.

A key element in the characterization of the relative state of two coupled automata is given by the difference automaton. By definition, if the states of cell i in the two automata are $\sigma_i^1(t)$ and $\sigma_i^2(t)$, the state $\delta_i(t)$ of the same cell in the difference automaton is calculated as the Boolean difference between $\sigma_i^1(t)$ and $\sigma_i^2(t)$, namely,

$$\delta_i(t) = \sigma_i^1(t) \oplus \sigma_i^2(t) = |\sigma_i^1(t) - \sigma_i^2(t)| \,. \tag{16}$$

The average occupation, or density, of the difference automaton,

$$D(t) = \frac{1}{N} \sum_{i=1}^{N} \delta_i(t) \,, \tag{17}$$

provides a suitable "macroscopic" measure of the distance between the two coupled automata. In fact, it coincides with the Hamming distance [Wolfram, 1983] between the Boolean vectors $\boldsymbol{\sigma}^1(t)$ and $\boldsymbol{\sigma}^2(t)$.

3.1. *Coupled cellular automata*

Since elementary cellular automata admit a straightforward graphical representation, they constitute a convenient starting point for a qualitative exploration of the joint evolution of coupled automata. We choose to analyze in detail the case of two coupled cellular automata whose individual evolution is given by rule 150 (Table 1). Rule 150 gives rise to complex evolution patterns, with nonperiodic behavior for $N \to \infty$, and may therefore be classified as chaotic. It must be pointed out that rule 150 is, in a sense, pathological. In fact, it happens to belong to the class of *additive* rules [Wolfram, 1983], since its action can be given in terms of the Boolean sum of the neighborhood

Table 1. Action of rule 150 on the eight possible neighborhoods of site i. This rule assigns a 0 if the number of ones in the neighborhood is even, and a 1 otherwise.

$\sigma_{i-1}(t), \sigma_i(t), \sigma_{i+1}(t)$	$\sigma_i(t+1)$
0, 0, 0	0
0, 0, 1	1
0, 1, 0	1
0, 1, 1	0
1, 0, 0	1
1, 0, 1	0
1, 1, 0	0
1, 1, 1	1

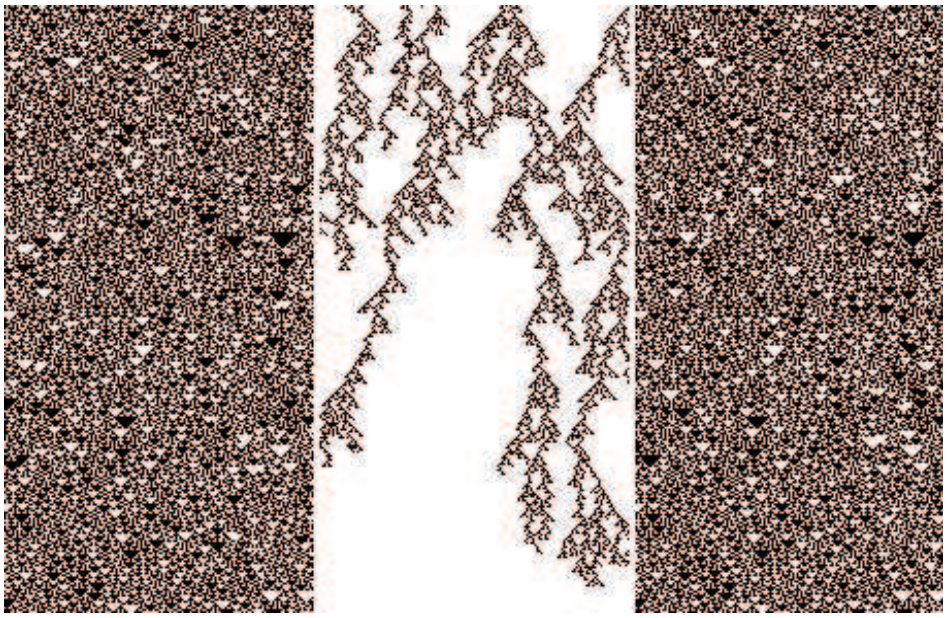

Fig. 3. Evolution of two cross-coupled automata, with rule 150 and coupling probability $q = 0.36$. Lateral columns show 300 steps for a 150-cell zone of the two automata, and the central column shows the corresponding difference automaton.

states: $f_{150}(\sigma_{i-1}, \sigma_i, \sigma_{i+1}) = \sigma_{i-1} \oplus \sigma_i \oplus \sigma_{i+1}$. This property implies, in particular, that — in the absence of coupling — the difference automaton of two automata evolving with rule 150 is also an elementary automaton, governed by the same rule. For other elementary automata, on the contrary, the difference automaton is typically *not* governed by an elementary rule.

This peculiarity of rule 150 has an important operational advantage. Indeed, in numerical realizations, instead of tracking the two coupled automata, it is possible to directly calculate the evolution of the difference automaton. Coupling is introduced as an additional process by which, with probability q, each site of the difference automaton in state 1 — which would correspond to different states in the homologous sites of the original coupled automata– is changed to 0. The particular nature of rule 150, on the other hand, does not introduce anomalies in the kind of features we are interested in, i.e. synchronization properties. Therefore, this rule is an ideal instance for the numerical investigation of our system.

3.1.1. *Numerical study of the synchronization transition*

Figure 3 shows, in the lateral columns, the evolution of two coupled cellular automata with $q = 0.36$, together with the corresponding difference automaton in the central column. Each line corresponds to the state at a given time step, and time proceeds downwards. White and black dots stand for the states 0 and 1, respectively. The plot begins at a stage where the difference automaton already reveals a high degree of synchronization (white areas). Complex branching structures are seen to propagate in a diffusive-like way, gradually disappearing as time elapses. Eventually, at the very last steps shown in the figure, the difference automaton reaches a homogeneous state, $\delta_i = 0$ for all i, and the two coupled automata attain full synchronization.

In Fig. 4, we present a more detailed illustration of the difference automaton for lower values of the coupling probability q, ranging from $q = 0$ to $q = 0.35$. Synchronization occurs first in small localized domains, which disappear after a few time steps. As q grows, however, synchronization domains increase in size and, at the same time, become more persistent. Finally, at the threshold of full synchronization, they reach sizes similar to that of the whole system.

As advanced above, a quantitative "macroscopic" characterization of the mutual state of the two coupled automata is given by the Hamming distance $D(t)$, introduced in Eq. (17). Figure 5 shows $D(t)$ as a function of time for two 2^{11}-cell automata with periodic boundary conditions, evolving with

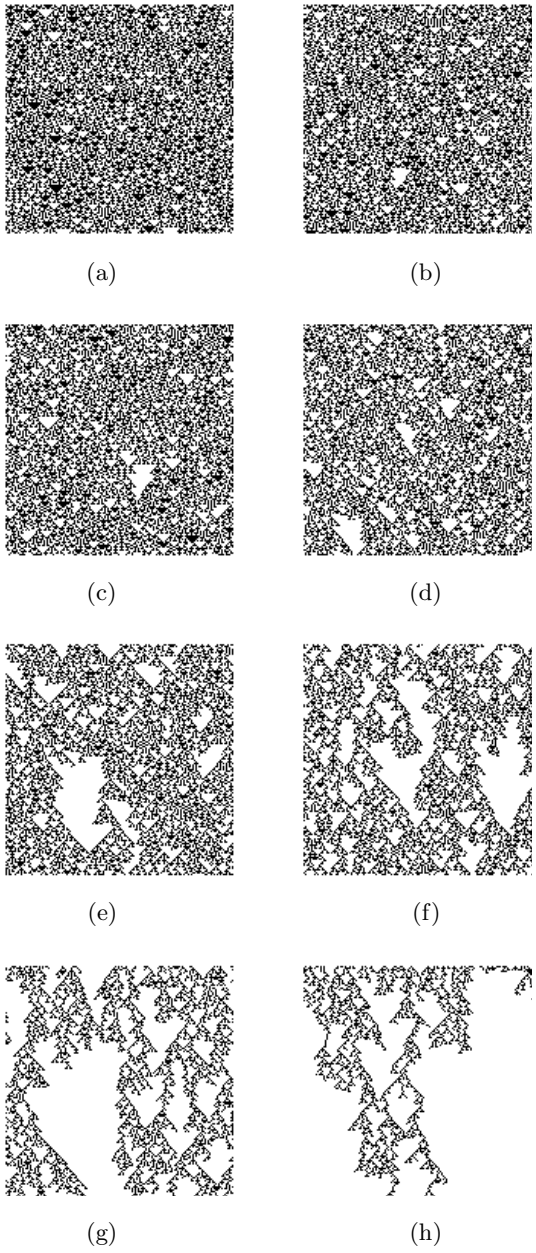

Fig. 4. Evolution of the difference automaton for rule 150 and different values of the coupling probability: (a) $q = 0$, (b) $q = 0.05$, (c) $q = 0.1$, (d) $q = 0.15$, (e) $q = 0.2$, (f) $q = 0.25$, (g) $q = 0.3$, and (h) $q = 0.35$.

rule 150 for different coupling probabilities. Each curve has been obtained from an average over 10^3 realizations. For small values of q the average density approaches asymptotically a finite level. Meanwhile, for large coupling probabilities it decreases exponentially at first, and then drops to zero at a finite time. At intermediate values, one finds a power-law decay of the density [Grassberger, 1999], $D(t) \sim t^{-\gamma}$ with $\gamma \approx 0.16$ (see inset in Fig. 5). Up to our numerical precision, the time range of power-law decay has maximal length for a coupling probability $q_c = 0.32115 \pm 0.00002$. This critical value is identified with the transition to full synchronization for rule 150.

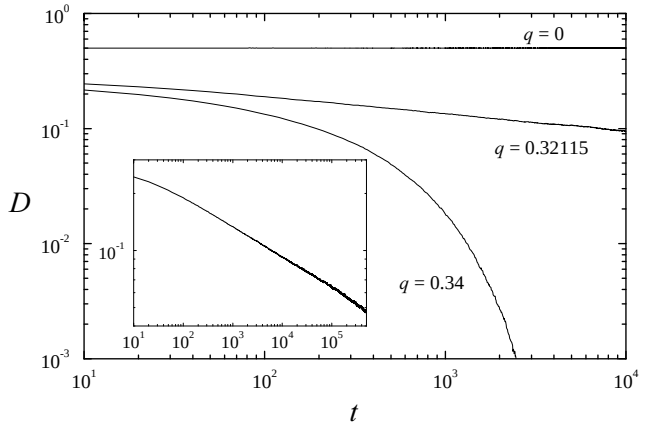

Fig. 5. Time evolution of the Hamming distance $D(t)$ between two 2^{11}-cell automata with rule 150, averaged over 10^3 realizations, for three coupling probabilities. The inset shows $D(t)$ at the critical coupling $q_c = 0.32115$ over a longer time range.

The critical-phenomenon nature of the synchronization transition becomes apparent by introducing the asymptotic density $D = \lim_{t\to\infty} D(t)$ as an order parameter. Dots in Fig. 6 show the average value of D over 10^4 time steps in 10^3 realizations for rule 150. After a smooth decay for low coupling probabilities, the average asymptotic density $\langle D\rangle$ drops abruptly to zero at q_c. This behavior suggests a functional form, just below the transition, given by

$$\langle D\rangle = A|q - q_c|^{\beta} . \qquad (18)$$

Linear fitting of $\ln\langle D\rangle$ versus $\ln|q - q_c|$ yields $\beta = 0.274 \pm 0.001$. The other two data sets in Fig. 6 illustrate the case of different evolution rules. Specifically, they correspond to rules 18 and 22, which are not additive. Despite the differences in the dependence for small q and the considerable dispersion in the critical coupling probability q_c at which synchronization starts — which is most plausibly related to differences in the Lyapunov exponents [Bagnoli & Rechtman, 1999] — the overall qualitative behavior is quite similar. The same is observed for other chaotic elementary evolution rules. Moreover, one finds that, within the numerical precision, the critical exponent β is the *same* for all these rules. This seems to indicate that, in all these cases, the synchronization transition

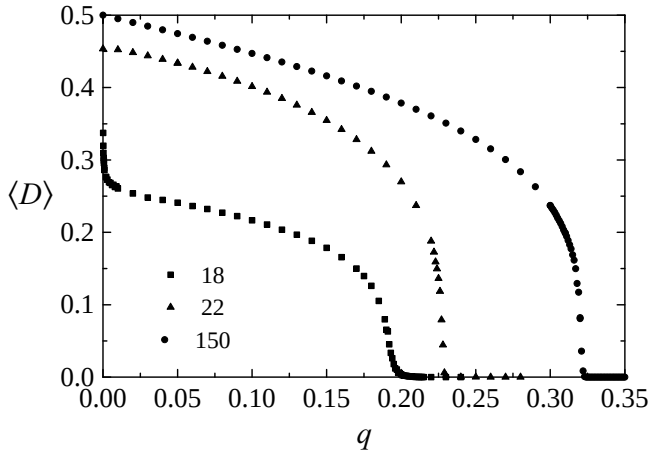

Fig. 6. Average asymptotic Hamming distance $\langle D\rangle$ as a function of the coupling probability q, for rules 18, 22, and 150. Averages were calculated over 10^4 steps in series of 10^2 realizations, for 2^{10} to 2^{13}-cell automata.

belongs to the same universality class. It has been argued [Grassberger, 1999] that it coincides with the universality class of random directed percolation, where $\beta \approx 0.276$.

3.1.2. *Analytical approaches*

It is quite natural to ask whether the synchronization transition occurring in cross-coupled elementary cellular automata admits an analytical description similar to that given for coupled differential equations. At a phenomenological level, in fact, such a description is possible if one accepts that the evolution of the Hamming distance $D(t)$ of two uncoupled automata is governed, at least in the large-size limit $N \to \infty$, by a deterministic equation $D(t+1) = \phi[D(t)]$. In such a case, it is easy to show that coupling introduces an additional factor in the evolution equation:

$$D(t+1) = (1-q)\phi[D(t)]\,. \tag{19}$$

The asymptotic Hamming distance, therefore, satisfies $D = (1-q)\phi(D)$. From this relation, and taking into account Eq. (18), we obtain

$$\begin{aligned}\phi(D) &= \frac{D}{1-q_c+(D/A)^{\beta^{-1}}} \\ &\approx \frac{D}{1-q_c} + \mathcal{O}[D^{1+\beta^{-1}}]\,. \end{aligned} \tag{20}$$

This gives the approximate form of $\phi(D)$ near the synchronization transition, where $D \approx 0$.

An analytical description at a more "microscopic" level should be able to yield, without any *a priori* assumption on the critical behavior of the system, an explicit form for the function $\phi(D)$. For the case of additive rules, where the rule governing the evolution of the difference automaton is known, the approach is quite intuitive from a probabilistic viewpoint. In fact, the Hamming distance $D(t)$ can be interpreted as the probability that the state of any cell in the difference automaton is 1 at time t. Therefore, $D(t+1)$ can be calculated as a function of $D(t)$ in the form of an evolution equation for such probability. This, however, requires to assume some degree of decorrelation between the states of individual cells. For instance, in the crudest approximation, it can be supposed that cells are completely uncorrelated. In this case, the probability $D(t+1)$ that a cell is in state 1 at step $t+1$ is simply given by the probability $D(t)$ of being in state 1 at step t times the probability of remaining in that state, plus the probability $1-D(t)$ of being in state 0 at step t times the probability of changing from 0 to 1. The transition probabilities involved in this calculation are directly provided by the evolution rule of the difference automaton. For rule 150, for instance, the probabilities of remaining in state 1 and of changing from 0 to 1 are both equal to 1/2 (see Table 1). Though this lowest-order approximation is not expected to give a satisfactory description, the same arguments can in principle be extended from single cells to uncorrelated three-cell neighborhoods, five-cell neighborhoods, and so on. Now, it can be easily verified that, as far as the correlation length is supposed to be finite, any such approximation produces a polynomial form for $\phi(D)$. Comparing with Eq. (20), we realize that a polynomial evolution law for $D(t)$ is unable to explain the critical behavior observed in numerical realization of the system. The situation worsens, of course, if nonadditive rules are considered, for which the difference automaton is not elementary.

The failure of the hypothesis of finite-length correlation evidences the strong effect of the propagation of information along the highly ordered geometry of cellular automata. It establishes long-range connections between cells, in the form of dynamical correlations that ultimately pervade the whole system. These correlations are revealed, in the dynamics of independent automata, by the complex spatiotemporal structures originated by certain evolution rules. We see here that they also have a relevant role in the coevolution of coupled

automata, in particular, determining the nontrivial critical-phenomenon nature of the synchronization transition. In the next section, we show that the situation is quite different for Kauffman networks. The inherent randomness of these disordered automata eliminates the effect of correlations, and a successful analytical description of their synchronization properties, along the lines sketched above, becomes feasible.

3.2. *Coupled Kauffman networks*

3.2.1. *The annealed model*

In the case of Kauffman networks — where, in contrast with elementary cellular automata, the neighborhood of each cell and the corresponding evolution rule is chosen at random — the evolution of the Hamming distance between two automata has been explicitly considered in the frame of damage-spreading problems. The so-called annealed model [Derrida & Pomeau, 1986; Derrida & Weisbuch, 1986] gives an unexpectedly good analytical description of $D(t)$ in the limit of large size, $N \to \infty$. This model assumes that the K neighbors of each cell, as well as the Boolean function that defines its evolution, are randomly changed at each time step. In other words, an entirely different realization of the network is used at each step. Possible spatiotemporal correlations generated during the evolution are therefore being continuously erased. The success of the annealed model reveals, in fact, that in large Kauffman networks such correlations are negligible or directly absent.

Suppose now that one has two identical Kauffman networks, with the same connections and rules. They are fed with different initial conditions, and let to evolve in time. The *overlap* $a(t)$ between the networks is defined as the fraction of homologous cells that are in the same state at time t. Clearly, we have $a(t) = 1 - D(t)$. Within the annealed model, it is possible to calculate the time evolution of the overlap and, thus, of $D(t)$. At each time, connections and rules are reassigned to each cell, but the same changes are applied to both networks, keeping their structure and local dynamical rules identical. The probability for a cell having all its K inputs coming from homologous sites in the same state in both networks is $a(t)^K$. At the next time step, consequently, such cell will be in the same state in both networks, no matter the evolution rule chosen for it. Hence, there is a fraction $a(t)^K$ of homologous sites whose state will coincide at $t+1$. The remaining $[1 - a(t)^K]N$ homologous cells still have a probability of reaching identical states. In fact, even if the state of the neighborhoods of a given cell are different in the two networks, it may happen that the evolution rule assigns the same output to them. In terms of the bias p of the Kauffman network, defined in Sec. 2, the probability of getting two homologous cells in the same state σ_i is $(1-p)^2$ for $\sigma_i = 0$ and p^2 for $\sigma_i = 1$. Consequently, the overlap at time $t+1$ can be written as $a(t+1) = a(t)^K + [1 - a(t)^K][p^2 + (1-p)^2]$. For the Hamming distance, this implies

$$\begin{aligned} D(t+1) &= 2p(1-p)(1 - [1 - D(t)]^K) \\ &\equiv \phi[D(t)]\,. \end{aligned} \tag{21}$$

The annealed model, thus, provides an explicit form for the function $\phi(D)$. As in the case of elementary cellular automata, the effect of coupling is represented by an extra factor $1-q$ in the evolution law, as in Eq. (19) [Morelli & Zanette, 2001].

The equation for the equilibrium Hamming distance between two coupled automata,

$$D = 2p(1-p)(1-q)[1 - (1-D)^K]\,, \tag{22}$$

has a trivial solution at $D = 0$, which corresponds to the fully synchronized state. A second solution D^* in the interval $(0, 1)$ is found for sufficiently low values of the coupling probability q, if the condition $2p(1-p)K \geq 1$ is fulfilled. This is precisely the condition for the individual dynamics of each Kauffman network to be chaotic (cf. Sec. 2). For small q, D^* is a stable equilibrium whereas the trivial equilibrium $D = 0$ is unstable. As q grows, D^* decreases and, at a critical coupling probability

$$q_c = 1 - [2p(1-p)K]^{-1} \tag{23}$$

it equals zero. For $q > q_c$, D^* is negative and becomes an unstable equilibrium. At the same time, $D = 0$ becomes stable. We thus have a transcritical bifurcation at q_c which, clearly, corresponds to the synchronization transition.

The explicit form of D^* as a function of q cannot be given for arbitrary K, as it would imply finding the roots of a polynomial of the $(K-1)$th degree. For $K = 3$ — a case considered below in the numerical realizations — one finds

$$D^* = \frac{3}{2} - \frac{1}{2}\left[-3 + \frac{2}{p(1-p)(1-q)}\right]^{1/2}. \tag{24}$$

For any value of K, however, it is possible to give the following approximate form of D^* near q_c:

$$D^* \approx \frac{4K}{K-1}\, p(1-p)|q-q_c|\,. \qquad (25)$$

Within the annealed approximation, consequently, the synchronization transition has a critical exponent $\beta = 1$ [cf. Eq. (18)].

3.2.2. *Numerical results*

Numerical realizations of two Kauffman networks coupled according to the scheme described in Sec. 3 show that the lowest coupling probability at which the networks synchronize is systematically lower than that predicted by the annealed model. For $K = 3$ and $p = 1/2$, for instance, two 2^{10}-cell networks are found to synchronize from $q \approx 0.29$, whereas the annealed model yields $q_c = 1/3 \approx 0.33$. Discarding the effects of correlations, discussed for cellular automata, a possible origin for this discrepancy is to be found in finite-size effects. Indeed, the annealed model is expected to be valid in the limit $N \to \infty$. Close inspection of the joint evolution of finite-size coupled networks shows that the system may in fact undergo *spurious* synchronization for coupling probabilities below q_c [Morelli & Zanette, 2001]. Due to the stochastic nature of the coupling mechanism — and especially near q_c, where only a few pairs of homologous cells are in different states — it is likely that a fluctuation brings the two networks to exactly the same state. They thus synchronize and, from then on, their states are identical.

Spurious synchronization can be avoided by adding a small amount of noise to the dynamics. With this new ingredient, exact synchronization is not possible anymore but — as long as the noise is kept at low levels — the overall dynamics is only slightly affected. Noise is introduced in numerical realizations as an additional step in the evolution. Once the individual dynamics and the coupling algorithm have acted, the state of each cell in one of the networks is flipped with probability η. It can be readily shown that noise enters the annealed model modifying the evolution of the Hamming distance as

$$D(t+1) = (1-\eta)(1-q)\phi[D(t)] + \eta\{1-(1-q)\phi[D(t)]\} \qquad (26)$$

where $\phi(D)$ is defined in Eq. (21).

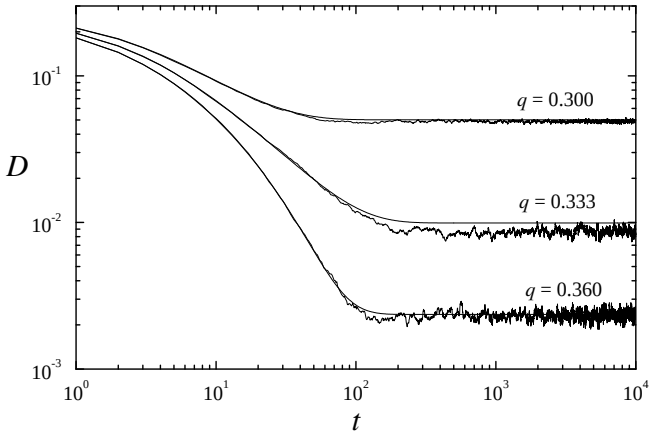

Fig. 7. Time evolution of the Hamming distance $D(t)$ between two 2^{13}-cell Kauffman networks ($K = 3, p = 1/2$) for three different coupling probabilities near the critical value predicted by the annealed model, $q_c = 1/3$, averaged over 10^2 realizations. The noise level is $\eta = 10^{-4}$. The curves correspond to the solution of the annealed model, Eq. (26), for the same couplings and noise level.

Figure 7 shows the evolution of $D(t)$ for two coupled 2^{13}-site networks ($K = 3$, $p = 1/2$) close to the critical coupling, with a noise level $\eta = 10^{-4}$ — such that, on the average, the state of approximately one site is flipped at each step. The curves stand for the iterative solution to Eq. (26). The agreement between numerical realizations and the annealed model is, generally, very good both in the transients and in the long-time evolution. The only noticeable systematic difference regards the asymptotic Hamming distance precisely at the critical coupling probability, where the value predicted by the annealed model is somewhat above the observed values. This remnant difference results in a genuine finite-size effect — not related with spurious synchronization. This is shown in Fig. 8, where the curve stands for the equilibrium Hamming distance predicted by the annealed model, Eq. (26), with $\eta = 10^{-4}$, and the dots are the measured numerically for different network sizes and the same noise level. For $N = 2^{10}$ and 2^{14} the agreement is excellent, except near the critical coupling.

A careful study of remnant size effects shows that the difference between the asymptotic Hamming distance predicted by the annealed model and observed in numerical realizations decreases as N^{-1} over a wide range of coupling probabilities. A statistical description of the dynamics of the coupled networks, based on an ergodic-like assumption about their asymptotic evolution, has been advanced to

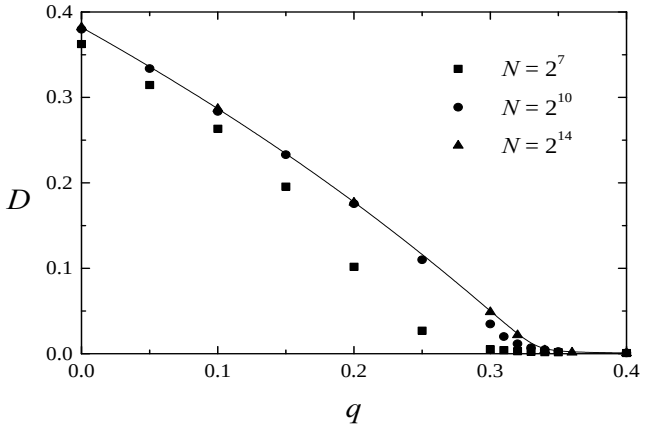

Fig. 8. Asymptotic Hamming distance between two Kauffman networks ($K = 3, p = 1/2$) as a function of the coupling probability, for three different sizes and a noise level $\eta = 10^{-4}$. The curve stands for the prediction of the annealed model for the same noise level.

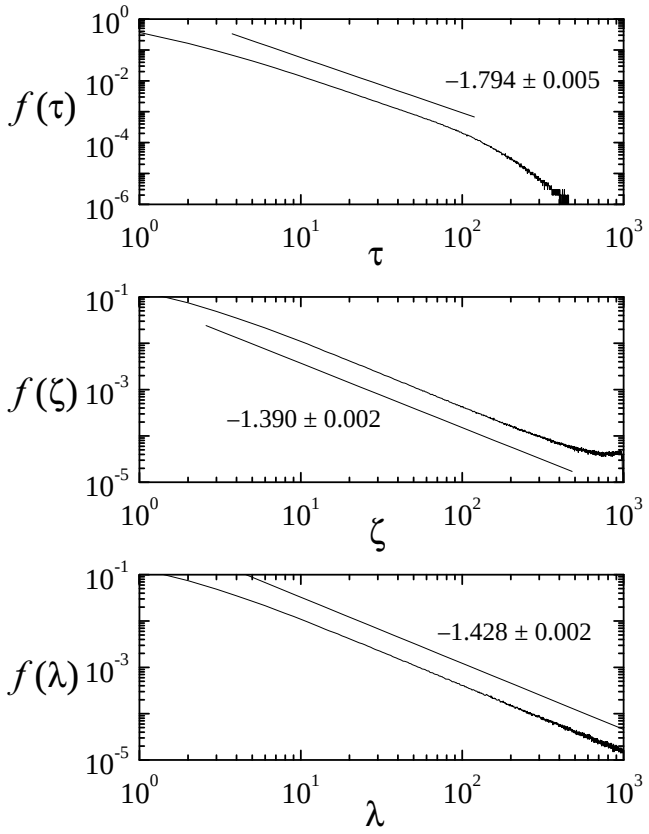

Fig. 9. Distribution of avalanche sizes in the difference automaton of two 2^{10}-cell Kauffman networks ($K = 3, p = 1/2$) at $q = 0.3333$. The normalized frequency f is shown for the avalanche duration τ, the number of affected cells ζ, and the avalanche intensity λ. Straight lines correspond to least-square fittings in the power law regimes. Their slopes are indicated in each plot.

explain such dependence on the system size [Morelli & Zanette, 2001].

We have already mentioned that the annealed model predicts a critical exponent equal to unity for the equilibrium Hamming distance as a function of the coupling probability [see Eq. (25)]. A more complete characterization of the critical behavior at q_c is given by the properties of damage spreading [Derrida & Pomeau, 1986; Derrida & Weisbuch, 1986; Bagnoli & Rechtman, 1999]. Consider two fully synchronized Kauffman networks in the chaotic phase, during their asymptotic evolution. All the cells in the difference automaton are in the same state 0. Now, a defect is introduced by flipping the state of a single cell in one of the networks — which amounts to flipping the state of the corresponding cell in the difference automaton from 0 to 1. While for $q < q_c$ the defect is expected to propagate due to the underlying chaotic-like evolution, for $q > q_c$ the effect of coupling dominates over the inherently unstable dynamics and the defect is rapidly suppressed. At the critical point, the defect originates an avalanche of irregular duration and extent. In a finite system, ultimately, the avalanche terminates at a finite time.

The avalanche size can be quantified by its total duration τ, by the number ζ of cells affected at least once during the avalanche, and by the avalanche intensity λ, which is given by the number of affected cells weighted by the number of steps in which each of them was affected. Figure 9 shows histograms for τ, ζ, and λ, constructed from measurement of 10^7 avalanches in 2^{10}-cell networks with $K = 3$, $p = 1/2$, and $q = 0.3333$. In all the cases, there is a well-defined regime of power-law decay with nontrivial exponents. These power laws are an additional clue to the criticality of the synchronization transition in coupled Kauffman networks.

4. Synchronization of Other Extended Systems

Although cellular automata and, especially, Kauffman networks seem to be the only class of spatially extended systems whose synchronization properties under the effect of cross-coupling have been systematically studied — perhaps due to the feasibility of their computational implementation — a few other kinds of extended systems have also been analyzed, though in less detail, in the literature. In this section we present a short summary of the main results on two of those systems.

4.1. *Complex Ginzburg–Landau equation*

The one-dimensional complex Ginzburg–Landau equation,

$$\partial_t A = \mu A + (1+i\alpha)\partial_x^2 A - (1+i\beta)A|A|^2\,, \quad (27)$$

describes the evolution of the (complex) amplitude $A(x,t)$ of a continuous array of nonlinear oscillators near a Hopf bifurcation. Depending on the parameters μ, α and β, the solutions display a wealth of behaviors, ranging from frozen and regularly oscillatory evolution to chaotic dynamics. Two complex Ginzburg–Landau equations have been considered under the following coupling scheme [Amengual *et al.*, 1997]:

$$\begin{aligned}\partial_t A_{1,2} = {} & \mu A_{1,2} + (1+i\alpha)\partial_x^2 A_{1,2} \\ & - (1+i\beta)A_{1,2}(|A_{1,2}|^2 + \varepsilon|A_{2,1}|^2)\,. \quad (28)\end{aligned}$$

Coupling is weighted by the parameter ε; for $\varepsilon = 0$ the two equations are uncoupled. Note however that this form of coupling is *not* of the same type considered in Secs. 1 and 2. In fact, Eq. (28) do not reduce to the form (27) for $A_1 = A_2$.

Synchronization properties of Eq. (28) have been studied in a regime where the system displays spatiotemporal intermittency. In this form of chaotic evolution, the amplitude exhibits localized structures that are created, move and then disappear in a disordered fashion, as time elapses. For small values of the coupling intensity ε it is observed that, as expected, A_1 and A_2 follows nearly independent evolution. As ε grows, however, the two coupled amplitudes become increasingly correlated. Specifically, it is observed that the zones where $|A_1|$ attains local maxima correspond to minima in $|A_2|$, and *vice versa*. At the same time, the intermittent spatiotemporal structures become, on the average, wider and more persistent. Eventually, going beyond a certain critical coupling intensity, the intermittent behavior is suppressed and the system falls in a frozen state with spatial domains where either A_1 or A_2 vanishes, while the other is constant. A quantitative analysis of this process reveals a form of *generalized* synchronization. As coupling becomes stronger, in fact, the system approaches a state with highly correlated amplitudes, where $|A_1|^2 + |A_2|^2 \approx \mu$. Beyond the critical coupling, either $|A_1| = 0$ and $|A_2| = \sqrt{\mu}$, or $|A_1| = \sqrt{\mu}$ and $|A_2| = 0$.

Let us also mention that the relevant issue of the synchronization properties of coupled *nonidentical* extended systems has been addressed in the frame of the complex Ginzburg–Landau equation [Boccaletti *et al.*, 1999]. In this case, the coupling scheme has been proposed to have the form

$$\begin{aligned}\partial_t A_{1,2} = {} & \mu A_{1,2} + (1+i\alpha_{1,2})\partial_x^2 A_{1,2} \\ & - (1+i\beta_{1,2})A_{1,2}|A_{1,2}|^2 \\ & + \varepsilon(A_{2,1} - A_{1,2})\,. \quad (29)\end{aligned}$$

This scheme coincides with that considered in Secs. 1 and 2, except for the fact that, for $\varepsilon = 0$, the uncoupled equations are different (if $\alpha_1 \neq \alpha_2$ and/or $\beta_1 \neq \beta_2$), thus representing nonidentical systems. The main result for this variant is that small mismatches in the parameters α and β lead the system to approach — though not to completely reach — a state of full synchronization, so that $A_1 \approx A_2$. For larger mismatches, on the other hand, *phase* synchronization is observed [Rosemblum *et al.*, 1996; 1997], where an approximate locking of the phases of A_1 and A_2 occurs, while their moduli remain uncorrelated.

4.2. *Neural networks*

We have already mentioned in the Introduction that synchronization in neural systems is an essential aspect of their functions, ranging from information-coding processes to pathological behavior. Whereas the joint evolution of coupled model neurons has been analyzed in detail in a series of publications (see, for instance, [Golomb *et al.*, 1992; Wang *et al.*, 1993] and the review by [Abarbanel *et al.*, 1996]), the dynamics of cross-coupled neural networks have attracted less attention. It has however to be stressed that highly correlated neural activity over vast portions of the brain, as observed for instance during epileptic seizures, should be associated with mutual synchronization of full neural networks rather than of individual neurons.

Mutual synchronization of a globally cross-coupled *ensemble* of identical neural networks has been studied using the following model [Zanette & Mikhailov, 1998b]:

$$x_k^i(t+1) = (1-\varepsilon)\Theta(h_k^i) + \varepsilon\Theta\left(\sum_j h_k^j\right) \quad (30)$$

[cf. Eq. (4)]. Here, $x_k^i \in [0,1]$ is the state of the kth neuron in the ith network at time t, and

$h_k^i = \sum_m w_{km} x_m^i(t)$ is the signal arriving at this neuron from all the other neurons of the same network, with w_{km} the connection weights (the same for all networks). The neuron response is characterized by the sigmoidal function $\Theta(h)$. The first term in the right-hand side of Eq. (30) represents the individual response of a neuron to the signal received from other elements in its own network. The second term depends on the global signal arriving from the homologous neurons in all the networks of the ensemble, and is weighted by the coupling intensity ε.

Generally, for asymmetric connection weights, $w_{km} \neq w_{km}$, the individual dynamics of these neural networks is chaotic. Synchronization properties have been analyzed in such regime. It has been shown that the synchronization transition is preceded, as the coupling intensity grows, by a stage of clustering, exactly as observed for chaotic maps [Kaneko, 1989, 1994]. The ensemble becomes divided into several clusters with different — typically chaotic — trajectories. Within each cluster, however, the networks are fully synchronized. The synchronization transition itself is qualitatively similar to that of globally coupled maps.

An interesting variant regards the case where the coupling between networks does not affect all the neurons. This is represented by the equations

$$x_k^i(t+1) = (1-\varepsilon\xi_k)\Theta(h_k^i) + \varepsilon\xi_k\Theta\left(\sum_j h_k^j\right), \quad (31)$$

where ξ_k represent random variables taking the values 0 or 1 with probabilities $1-p$ and p, respectively. Thus, only a fraction p of neurons in each network is sensitive to the global signal. In the parameter space (ε, p) three different phases are found. For small ε, as expected, no synchronization is observed. On the other hand, for large ε and large p there is full synchronization. Near $\varepsilon = 1$, in fact, full synchronization occurs for values of p as low as 0.3, which means that only 30% of global cross-coupling connections remain in the ensemble. These two zones are separated by an intermediate regime of clustering, where at least two networks are fully synchronized.

An important problem that remains to be studied in connection with coupled neural networks is that of synchronization of nonidentical elements. Considering nonidentical cross-coupled networks could prove to be necessary to explain the variations in the dynamical properties — specifically, the change from chaotic to almost-periodic evolution — that accompany the appearance of synchronization in real neural activity.

5. Conclusion

As a conclusion to this brief review, let us first comment on the main similarities and differences found in the synchronization properties of spatially extended and zero-dimensional chaotic dynamical systems. We begin pointing out that two cross-coupled identical extended systems undergo a sharp transition to full synchronization as the intensity of coupling is increased, exactly as observed to happen for a pair of coupled zero-dimensional systems, as long as coupling implies a relaxation towards a common dynamical state. This similarity holds even when coupling is inherently stochastic for extended systems such as cellular automata and Kauffman networks, and deterministic for zero-dimensional systems. In both cases, the transition can be ascribed to the competing effect of two mechanisms, namely, the intrinsic instability of the chaotic individual dynamics on one hand, and the mutual relaxation towards a common trajectory in phase space on the other. The critical-phenomenon nature of the synchronization transition is well described by the dependence of a suitable order parameter — measuring the average distance in phase space of the two individual trajectories — on the coupling intensity. In zero-dimensional systems, the synchronization transition is mediated by an intermittency regime. Just below the transition, the system alternates between long periods of quasi-synchronized evolution, where the states of the two coupled elements almost coincide, and sudden bursts of desynchronization [Kaneko, 1989]. In extended system, in contrast, the critical dynamics is characterized by *spatiotemporal* intermittency. This is well illustrated, in the case of cellular automata, by the dynamical structure of the difference automaton near the transition (see Figs. 3 and 4). While most of its cells are in state 0, there are localized regions in state 1, where the automata are unsynchronized. These localized structures are created by branching from other similar regions, evolve with time in a diffusive-like fashion, and eventually disappear. Note carefully that the presence of spatiotemporal intermittency does not imply intermittent temporal evolution in global quantities. In fact, the distance between the two automata — i.e. the density of

the difference automaton — evolves uniformly and does not exhibit the characteristic bursts of strong variation.

Comparison of the critical behavior at the synchronization transition for cross-coupled elementary cellular automata and Kauffman networks also reveals similarities and differences. In the two cases the order parameter D, given by the asymptotic Hamming distance between the coupled automata, behaves as $D \sim |q - q_c|^\beta$ near the transition. Both for cellular automata and for Kauffman networks the critical coupling probability q_c depends on the evolution rules, whereas the critical exponent β is universal. The value of β, however, is different for the two kinds of automata. While for elementary cellular automata one finds $\beta \approx 0.274$ — very close to the critical exponent of directed percolation [Grassberger, 1999] — for Kauffman networks the exponent is trivial, $\beta = 1$. This difference seems to be a direct consequence of the presence of disorder in the structure of Kauffman networks. In fact, it has been shown that cross-coupled *partially* disordered automata — whose structure is similar to the so-called small-world networks [Watts & Strogatz, 1998] — behave exactly as Kauffman networks even for very low levels of disorder [Morelli & Zanette, 2001]. The intrinsic randomness of Kauffman networks makes it possible to formulate an analytical approach based on the assumption of time decorrelation of their successive states — the annealed model [Derrida & Pomeau, 1986]. This approach has been successfully extended to the case of cross-coupled networks, showing that the synchronization transition is associated with a transcritical bifurcation, which explains the trivial exponent $\beta = 1$. In contrast, the ordered structure of cellular automata introduce long-range correlations that cannot be satisfactorily neglected at any order. These correlations are plausibly related to the nontrivial nature of the synchronization transition of cellular automata.

Two important aspects of synchronization phenomena have been studied in extended systems other than cellular automata and Kauffman networks. The first one regards the synchronization properties of cross-coupled nonidentical systems, in the case of the Ginzburg–Landau equation [Boccaletti *et al.*, 1999]. For this system, generalized forms of synchronized evolution have been detected. The second aspect involves the consideration of identical extended systems when coupling does not affect the whole system, but is localized in certain spatial domains. Under these conditions, full and partial synchronization has been observed in cross-coupled neural networks [Zanette & Mikhailov, 1998b]. In view of the potentiality of automata as powerful abstract representations of complex systems and as models of specific natural objects, the study of such aspects in connection with these discrete extended systems would constitute a fruitful line of future work.

Acknowledgments

Fruitful collaboration and/or discussion with Guillermo Abramson, Stefano Boccaletti, Hilda Cerdeira, Jack Hudson, Susanna Manrubia and Alexander Mikhailov is gratefully acknowledged.

References

Abarbanel, H. D., Rabinovich, M. I., Selverston, A., Bazhenov, M. V., Huerta, R., Sushchik, M. M. & Rubchinskii, L. L. [1996] "Synchronization in neural assemblies," *Phys. Usp.* **39**(4), 337–362.

Abramson, G. [2000] "Long transients and cluster size in globally coupled maps," *Europhys. Lett.* **52**(6), 615–619.

Amengual, A., Hernández-García, E., Montagne R. & San Miguel, M. [1997] "Synchronization of spatiotemporal chaos: The regime of coupled spatiotemporal intermittency," *Phys. Rev. Lett.* **78**(23), 4379–4382.

Bagnoli, F. & Rechtman, R. [1999] "Synchronization and maximum Lyapunov exponents of cellular automata," *Phys. Rev.* **E59** (2), R1307–R1310.

Bastolla, U. & Parisi, G. [1996] "Closing probabilities in the Kauffman model: An annealed computation," *Physica* **D98**(1), 1–25.

Bastolla, U. & Parisi, G. [1998a] "Relevant elements, magnetization and dynamical properties in Kauffman networks," *Physica* **D115**(3 & 4), 203–218.

Bastolla, U. & Parisi, G. [1998b] "The modular structure of Kauffman networks," *Physica* **D115**(3 & 4), 219–233.

Boccaletti, S., Bragard, J., Arecchi, F. T. & Mancini, H. [1999] "Synchronization in nonidentical extended systems," *Phys. Rev. Lett.* **83**(3), 536–539.

Buck, J. & Buck, E. [1976] "Synchronous fireflies," *Sci. Am.* **234**(5), 74–85.

Crisanti, A., Falcioni, M., & Vulpiani, A. [1996] "Broken ergodicity and glassy behavior in a deterministic chaotic map," *Phys. Rev. Lett.* **76**(4), 612–615.

Derrida, B. & Pomeau, Y. [1986] "Random networks of automata: A simple annealed approximation," *Europhys. Lett.* **1**(2), 45–49.

Derrida, B. & Weisbuch, G. [1986] "Evolution of overlaps

between configurations in random Boolean networks," *J. Physique* **47**(8), 1297–1303.

Flyvbjerg, H. [1988] "An order parameter for networks of automata," *J. Phys. A: Math. Gen.* **21**(19), L955–L960.

Fujisaka, H. & Yamada, T. [1983] "Stability theory of synchronized motion in coupled oscillator systems," *Prog. Theor. Phys.* **69**(1), 32–47.

Golomb, D., Hansel, D., Shraiman, B. & Sompolinsky, H. [1992] "Clustering in globally coupled phase oscillators," *Phys. Rev.* **A45**(6), 3516–3530.

Grassberger, P. [1999] "Synchronization of coupled systems with spatiotemporal chaos," *Phys. Rev.* **E59**(3), R2520–R2522.

Heagy, J. F., Carroll, T. L. & Pecora, L. M. [1994] "Synchronous chaos in coupled oscillator systems," *Phys. Rev.* **E50**(3), 1874–1885.

Herrmann, H. J. [1989] "Cellular Automata," in *Nonlinear Phenomena in Complex Systems*, ed. Proto, A. N. (North-Holland, Amsterdam), pp. 151–199.

Kaneko, K. [1989] "Chaotic but regular posi-nega switch among coded attractors by cluster-size variation," *Phys. Rev. Lett.* **63**(3), 219–223.

Kaneko, K. [1990] "Globally coupled chaos violates the law of large numbers but not the central-limit theorem," *Phys. Rev. Lett.* **65**(12), 1391–1394.

Kaneko, K. [1993] *Theory and applications of coupled map lattices* (Wiley, Chichester).

Kaneko, K. [1994] "Relevance of clustering to biological networks," *Physica* **D75**(1–3), 55–73.

Kauffman, S. A. [1969] "Metabolic stability and epigenesis in random constructed genetic nets," *J. Theor. Biol.* **22**(3), 437–467.

Kauffman, S. A. [1984] "Emergent properties in random complex automata," *Physica* **D10**(1 & 2), 145–156.

Kauffman, S. A. [1993] *The Origins of Order* (Oxford University Press, Cambridge).

Kuramoto, Y. [1984] *Chemical Oscillations, Waves, and Turbulence* (Springer, Berlin).

Manrubia, S. C. & Mikhailov A. S. [2001] "Globally coupled logistic maps as dynamical glasses," *Europhys. Lett.* **53**(4), 451–457.

Mikhailov, A. S. [1994] *Foundations of Synergetics I*, 2nd edition (Springer, Berlin).

Morelli, L. G. & Zanette, D. H. [1998] "Synchronization of stochastically coupled cellular automata," *Phys. Rev.* **E58**(1), R8–R11.

Morelli, L. G. & Zanette, D. H. [2001] "Synchronization of Kauffman networks," *Phys. Rev.* **E63**(3), 036204.

Murray, J. D. [1993] *Mathematical Biology*, 2nd edition (Springer, Berlin).

Néda, Z., Ravasz, E., Vicsek, T., Brechet, Y. & Barabási, A. L. [2000] "Physics of the rhythmic applause," *Phys. Rev.* **E61**(6), 6987–6992.

Perez, G., Pando-Lambruschini, C., Sinha, S. & Cerdeira, H. A. [1992] "Nonstatistical behavior of coupled optical systems," *Phys. Rev.* **A45**(8), 5469–5473.

Perez, G., Sinha, S., & Cerdeira, H. A. [1993] "Order in the turbulent phase of globally coupled maps," *Physica* **D63**(3 & 4), 341–349.

Rosemblum, M. G., Pikovsky, A. S. & Kurths, J. [1996] "Phase synchronization of chaotic oscillators," *Phys. Rev. Lett.* **76**(11), 1804–1807.

Rosemblum, M. G., Pikovsky, A. S. & Kurths, J. [1997] "From phase to lag synchronization in coupled chaotic oscillators," *Phys. Rev. Lett.* **78**(22), 4193–4196.

Strogatz, S. H. & Stewart, I. [1993] "Coupled oscillators and biological synchronization," *Sci. Am.* **269**(6), 68–75.

Walker, T. J. [1969] "Acoustic synchrony: Two mechanisms in the snowy tree cricket," *Science* **166**(3907), 891–894.

Wang, W., Perez, G. & Cerdeira, H. A. [1993] "Dynamical behavior of the firings in a coupled neuronal hboxsystem," *Phys. Rev.* **E47**(4), 2893–2898.

Wang, W., Kiss, I. S. & Hudson, J. L. [2000] "Experiments on arrays of globally coupled chaotic electrochemical oscillators: Synchronization and clustering," *Chaos* **10**(1), 248–256.

Watts, D. J. & Strogatz, S. H. [1998] "Collective dynamics of 'small-world' networks," *Nature* **393**(6684), 440–442.

Winfree, A. T. [1980] *The Geometry of Biological Time* (Springer, Berlin).

Wolfram, S. [1983] "Statistical mechanics of cellular automata," *Rev. Mod. Phys.* **55**(3), 601–644.

Wolfram, S. [1986] *Theory and Applications of Cellular Automata* (World Scientific, NY).

Zanette, D. H. & Mikhailov, A. S. [1998a] "Condensation in globally coupled populations of chaotic dynamical systems," *Phys. Rev.* **E57**(1), 276–281.

Zanette, D. H. & Mikhailov, A. S. [1998b] "Mutual synchronization in ensembles of globally coupled neural networks," *Phys. Rev.* **E58**(1), 872–875.

Zanette, D. H. & Mikhailov, A. S. [2000] "Dynamical clustering in large populations of Rössler oscillators under the action of noise," *Phys. Rev.* **E62**(6), R7571–R7574.